Agromet 39 (2): 95-106, 2025

Agromet
journal.ipb.ac.id/index.php/agromet
ISSN : 0126 - 3633

ECMWF SEAS5 Seasonal Rainfall Assessment: A Study Case in Papua

Steven Cahya Andika[1, 2], I Putu Santikayasa[1*], Donaldi Sukma Permana[2]

[1] Department of Geophysics and Meteorology, IPB University, Bogor, Indonesia.
[2] Center for Standardization Instruments MKG, Meteorological, Climatological, and Geophysical Agency, Jakarta, Indonesia

ARTICLE INFO

Received
03 June 2025

Revised
30 June 2025

Accepted for Publication
19 August 2025

Published
08 Desember 2025

doi: 10.29244/j.agromet.39.2.95-106

Correspondence:
I Putu Santikayasa
Department of Geophysics and Meteorology, IPB University, Dramaga Campus, Bogor, Indonesia 16680.

Email: ipsantikayasa@apps.ipb.ac.id

ABSTRACT

Papua, Indonesia's easternmost island, is prone to seasonal hydrometeo-rological disasters, necessitating high-quality climate forecasts for effective risk management. This study evaluates the performance of the European Centre for Medium-Range Weather Forecasts (ECMWF) Seasonal Forecast System 5 (SEAS5) in predicting seasonal (3-monthly) rainfall across Papua from 1982 to 2016, using the blended Climate Hazards group InfraRed Precipitation with in-situ rainfall data (CHIRP+Pos) as the observational reference. SEAS5 forecasts at 1 to 3 month lead times were assessed across seasons which defined as July-August-September (JAS), August-September-October (ASO), September-October-November (SON), and December-January-February (DJF), and El Niño-Southern Oscillation (ENSO) phases (El-Niño, La-Niña, Neutral), using Pearson correlation coefficient (Corr), root mean square error (RMSE), and Kling-Gupta Efficiency (KGE) metrics. Results show stronger SEAS5 skill in JAS–SON (Corr up to 0.939) compared to DJF-JFM (Corr as low as -0.208), with a robust ENSO-rainfall relationship in JJA-SON. SEAS5 performed best during El Niño, particularly in lowlands and exhibited greater variability skill during La Niña and Neutral phases. Benchmarking against a linear regression baseline showed SEAS5's superior Corr in 76.2% of grids but higher RMSE in 60.6%. Despite limitations in mountainous regions and at longer lead times, SEAS5 offers reliable forecasts for lowland areas during JAS-SON under El Niño, supporting opera-tional applications like drought preparedness and agricultural planning in the regions.

KEYWORDS

climate extreme, ENSO, model evaluation, topography, seasonal prediction

1. INTRODUCTION

Rainfall plays an important role in both agriculture and disaster management in Indonesia. Lack of rainfall is linked to crop yield losses, impacting agricultural productivity in various regions in Indonesia (Daymond et al., 2020; Viandari et al., 2022; Irawan et al., 2023). Heavy or prolonged rainfall on the other hand increases the risk of floods and landslides, combined with factors like topography, slope, and land-use (Muntohar et al., 2022; Sugianti et al., 2022; Ariyani et al., 2023; Rahayu et al., 2023). Previous study suggest that climate-induced disaster, such as El Niño-induced drought, occurred the most in Papua (Nurdiati et al., 2023). High-quality climate predictions are therefore essential for stakeholders to plan and mitigate disaster risks in Papua.

Rainfall variability in Indonesia is mainly affected by various climatic driver. These climatic drivers include El-Niño Southern Oscillation (ENSO) (Aldrian et al., 2007; Supari et al., 2018; Firmansyah et al., 2022), Indian Ocean Dipole (IOD) (As-syakur et al., 2014; Kurniadi et al., 2021), Asian-Australian monsoons (Aldrian and Dwi Susanto, 2003; Robertson et al., 2011; Mulsandi et al., 2024)and sub-seasonal events like Madden Julian Oscillation (MJO) (Wu et al., 2013). ENSO's influence

varies by region with stronger effects in eastern Indonesia (Villafuerte and Matsumoto, 2015; Supari et al., 2018; Kurniadi et al., 2021). This variability underscores the need for specific regional rainfall prediction to support local government for decision making and disaster preparedness.

ENSO influences rainfall in Papua, particularly during El Niño phase in dry season, with strong relationship established using coarse-resolution data-set (Nurdiati et al., 2023). ENSO affects moisture dynamics in Papua, with isotopic ratios linked to convective activity and ENSO (Permana et al., 2016). However, limited spatial coverage highlights the need of higher resolution dataset to improve regional analysis in Papua.

Accurate seasonal rainfall forecasting is crucial for Papua. ECMWF provides prediction of various climate variables, with version 5 (SEAS5) as its latest dynamical model offering improvement over S4 (Johnson et al., 2019a). Comparisons with other models showed that ECMWF's seasonal forecast was superior compared to National Centers for Environmental Prediction-Global Forecast System (NCEP-GFS) (Rodrigues et al., 2014; Wang et al., 2023). ECMWF S4 outperformed Climate Forecast System version 2 (CFSv2) in Indonesia (Muharsyah, 2020). SEAS5's rainfall prediction performed well in tropical South America with strong ENSO relationship (Gubler et al., 2020). Comprehensive assessment of SEAS5's performance particularly in Papua remains limited to date.

Despite the established rainfall-ENSO relationship in Papua, few studies have evaluated the performance of ECMWF's latest seasonal model, SEAS5, across seasons and ENSO phases with high-resolution data. This gap limits the development of reliable seasonal rainfall forecasts for disaster preparedness in Papua. The main objective of this study is to assess the SEAS5 model in Papua at different seasonal periods and ENSO phases.

2. MATERIALS AND METHODS

2.1 Study Area

Papua Island occupies the easternmost of Indonesia, which is geographically located on 0°20'N to 10°42'S and 131° to 141°10'E. It currently consists of five provinces: Papua Barat, Papua Tengah, Papua Pegunungan, Papua, and Papua Selatan. The island is divided from the east-southeast to the west-northwest by mountain ranges that exceed 3500 m above sea level (m asl), including the highest peak, Puncak Jaya (4884 m asl). Papua landmass is dominantly covered by tropical rainforest with wetlands along coastal and grassland area in the highlands (Permana et al., 2016). Topography varied in this land, with several mountain ranges in western (Arfak Mountains, with elevation ranges between 1,030–2,280 m (Pangau-Adam and Brodie, 2019) and middle part (Maoke Mountains) of it as shown by Figure 1. This area has annual precipitation about 2500-4000 mm (Prentice and Hope, 2007) with dry period during DJF and MAM, while wet period occurred on JJA and SON (Supari et al., 2018).

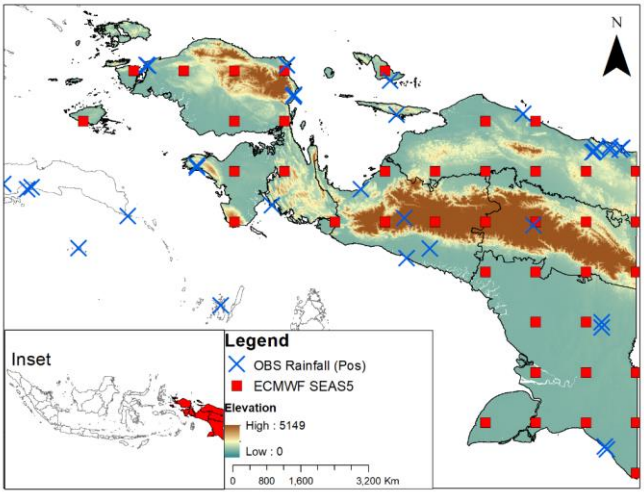

Figure 1. Location on this study. SEAS5 grid location is depicted in red square, while blue x mark depicts in-situ rainfall observational station used to create CHIRP+Pos. Shaded area shows elevation in meters, while black lines showed provincial administration.

2.2 Datasets

Data used in this study mainly consisted of 3 data-sets including CHIRP+Pos, Oceanic Niño Index (ONI), and SEAS5 rainfall prediction (Table 1). We used the same period from 1982-2016 for all datasets, align with SEAS5 data availability. CHIRP+Pos is blended data from satellite-derived rainfall data of Climate Hazards Center InfraRed Precipitation (CHIRP) (Funk et al., 2015) and in-situ rainfall data collected by BMKG using geo-statistics method. This data has been applied by data cleaning techniques to ensure high quality data, including data availability check (requiring at least 80% data completeness), gross error check, and advanced quality control which covered all

Table 1 Summary of data used

Data	Resolution		Source
	Temporal	Spatial	
CHIRP+ Pos	daily	0.05°x0.05°	BMKG
ECMWF SEAS5	monthly	1°x1°	Copernicus
ONI	3-monthly	-	NOAA

regions of Indonesia. The CHIRP+Pos data was used due to its fine resolution (0.05ºx0.05º) for further climatological analysis.

Seasonal forecast monthly used as predictor in this study derived from Climate Data Store (CDS) Copernicus which provides gridded free-to-access SEAS5 hindcast, also widely known as reforecast (Buontempo et al., 2022). This hindcast was derived from 25 ensemble models (referred as 'number' in the dataset) which have been improved compared to previous version (S4) of 15 members (Johnson et al., 2019b).

The determination of ENSO phases in this study was based from Oceanic Niño Index (ONI) (Supari et al., 2018). This index is calculated from 3-monthly moving average of Niño3.4 sea surface temperature, located on 120ºE-190ºE, 5ºN-5ºS from Extended Reconstructed Sea Surface Temperature version 5 (ERSSTv5) (Huang et al., 2017). Each ENSO phase was defined as follows: El Niño occurs when ONI value of ≥ +0.5 for 5 consecutive moving 3-months, while La Niña occurs when ONI value of ≤ -0.5, and neutral occurs when the ONI did not meet either El Niño or La Niña phase. The ONI is downloaded from Climate Prediction Center of National Oceanic and Atmospheric Adminis-tration's (CPC NOAA) website (Table 1).

2.3 Data Analysis

Data analysis in this study is divided in two main steps, data pre-processing and model performance assessment. Data preprocessing involved three major procedures. First, the ONI was calculated from 3-month moving average from both CHIRP+Pos and SEAS5 to ensure same temporal resolution. Seasonal rainfall was also calculated for climatological analysis and SEAS5 performance assessment. Second, we regridded CHIRP +Pos data into SEAS5 spatial resolution to maintain the spatial consistency. This is resulting total of 40 grids over Papua, thereby making the datasets more comparable for model assessment. Third, we calculated the mean ensemble hindcast data from 25-member of SEAS5 dataset.

The ensemble SEAS5 data has three different forecast lead times, divided into 1, 2, and 3 months yielding ensemble hindcast for each season. The forecast lead time is defined as number of months elapsed from initialization (Johnson et al., 2019b). For example, a 1 month lead time for forecast issued in November refer to forecast on DJF (Gubler et al., 2020). This ensemble approach was also been used to assess ECMWF's seasonal forecast in previous studies (Muharsyah, 2020; Ferreira et al., 2022).

After data preprocessing, we utilized three steps to assess SEAS5 performance. First, we calculated metrics scores commonly used in deterministic forecast including Pearson product-moment correlation coefficient (Corr), root mean square error (RMSE), and Kling-Gupta Efficiency (KGE) (Gupta et al., 2009; Chai and Draxler, 2014) for each lead times. Corr was calculated to assess the relationship between SEAS5 (prediction) and CHIRP+Pos (observation), with additional analysis of rainfall and ONI to contextualize ENSO influences to rainfall. The statistical metrics used are in idem equation.

$$Correlation = \frac{\sum_{i=1}^{n}(x_i-\bar{x})(y_i-\bar{y})}{\sqrt{\sum_{i=1}^{n}(x_i-\bar{x})^2}\sqrt{\sum_{i=1}^{n}(y_i-\bar{y})^2}} \quad (1)$$

$$RMSE = \sqrt{\frac{1}{n}\sum_{i=1}^{n}(\hat{y}_i - obs_i)^2} \quad (2)$$

$$KGE = 1 - \sqrt{(r-1)^2 + \left(\frac{\sigma_{pred}}{\sigma_{obs}} - 1\right)^2 + \left(\frac{\mu_{pred}}{\mu_{obs}} - 1\right)^2} \quad (3)$$

Second, we developed simple linear regression based on elevation as a predictor (x) to quantify the relationship between topography and SEAS5 performance using RMSE metric (y). The relationship was determined by the regression coefficient and coefficient determination or R^2 values of SEAS5 data over study area. Third, we compared the SEAS5 with a baseline linear model using 3-monthly moving average ONI as predictor, reflecting real world applicability as ONI data are available by the first week of the following month.

This study utilized Python version 3.8.18 with Pandas, Numpy, Xarray, Scikit-Learn, and Scipy for data manipulation and calculation (Hoyer and Hamman, 2017; Harris et al., 2020). Matplotlib, Seaborn, and Basemap modules were used for data visualization and mapping tool also QGIS 2.18 was used to map the study area.

3. RESULTS AND DISCUSSION

3.1 Seasonal Performance

The seasonal performance of SEAS5 was assessed using statistical metrics across all seasons in Papua with re-gridded CHIRP+Pos data to match the resolution, as shown in Figure 2. The higher correlation value occured during dry period in JJA-SON ranges from 0.40 to more than 0.80, while during wet period in DJF-MAM had lower correlation. During the wet period, particularly in DJF, 40-43% of grids over Papua showed non-significant values between CHIRP+Pos and SEAS5 data with low correlation (-0.45 to 0.20), marked with 'x' (Figure 2a). KGE established a similar pattern as correlation, with higher values occurred during dry period and vice versa (Figure 2b). Both correlation and KGE showed consistent low results in high-elevation areas, indicates local characteristics such as orographic precipitation affect predictive skill of SEAS5 (Chevuturi et al., 2021). This pattern underscores that SEAS5 underper-

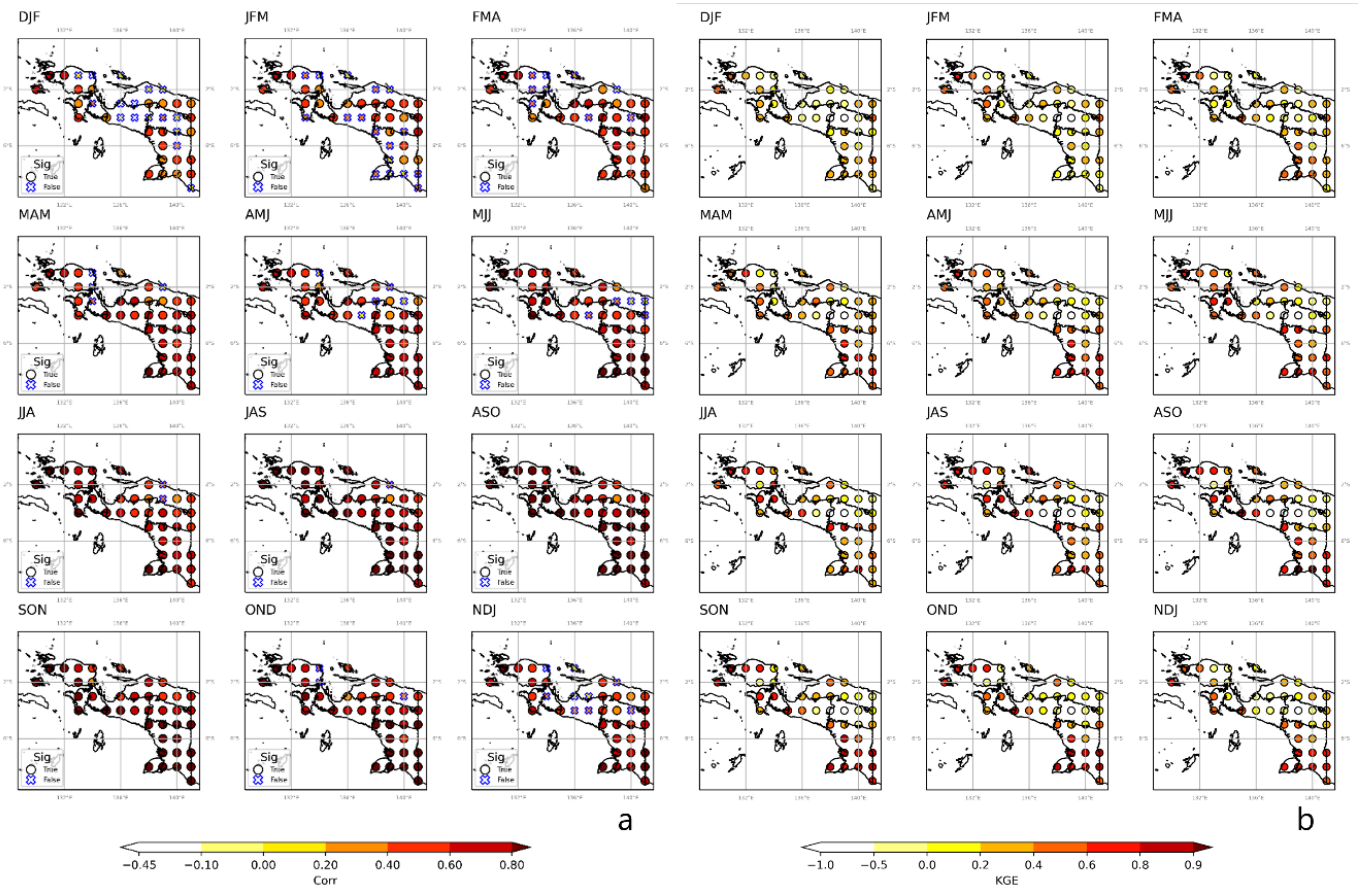

Figure 2 Seasonal performance of 3-month moving average of SEAS5 and CHIRP+Pos for 1 month lead time (a) Correlation; (b) Kling-Gupta Error (KGE). Shade showed metrics value with 'o' denotated significant value and 'x' is non-significant value for correlation

formed during wet period which has high rainfall variability.

The results of 3-month moving average for 1 month lead time showed good performance, dominant by significant values across all regions, except during DJF and JFM period. The correlation was highest in JAS to SON (up to 0.939) and lowest in DJF and JFM (as low as -0.208), with 40–43% of grids showing non-significant correlations particularly in high-elevation areas. KGE and RMSE confirmed poor performance in the Arfak and Maoke Mountains, with KGE values below -0.41 in some grids, indicating SEAS5 underperforms the climatological mean (Knoben et al., 2019).

Other result reveals distinct seasonal variations in SEAS5's skill over Papua observed by correlation (Corr), KGE, and RMSE. High Corr values consistently showed during the same period including JAS, ASO, and SON with higher median and mean also shorter interquartile range (IQR) (Figure 6) for each lead time. In contrast, DJF and NDJ exhibit lower mean and median Corr along with wider IQR, suggesting weaker and unstable SEAS5's skill. The large RMSE distribution in SON contributes to the similarly wide KGE, reflecting inconsistent and inaccurate rainfall prediction. High RMSE variability outweighs the relatively good Corr, leading to unstable KGE values. Wide IQRs of RMSE and KGE were observed on DJF and NDJ. With the established strong (weak) relationship of major climatic driver (ENSO) on SON (DJF), the weak performance of SEAS5 during DJF and NDJ implied major climate driver (regional mechanism) in Papua that SEAS5 succeeds (fails) to represent. Compared to boxplot (Figure 6) with most outliers occur mostly around mountainous areas. This further highlight regional mechanisms that affect SEAS5 skill in predicting rainfall.

3.2 ENSO-phase Performance

Results show that the skill of SEAS5 in Papua is modulated by ENSO phase, similar to previous studies (Abid et al., 2018; Palmer et al., 2004), particularly in lowland areas. The ENSO teleconnection is indicated by strong and significant correlation in ONI and rainfall (Figure 3). During all, El-Niño, and neutral phase, SEAS5 revealed good performance with high Corr values across the region, while the lowest Corr occurred during La-Niña evidenced by 30% grid showed non-significant correlation. The KGE demonstrated no significant difference between all phases with similar range in some high-elevation areas. Both Corr and KGE suggested best performance during El-Niño phase with

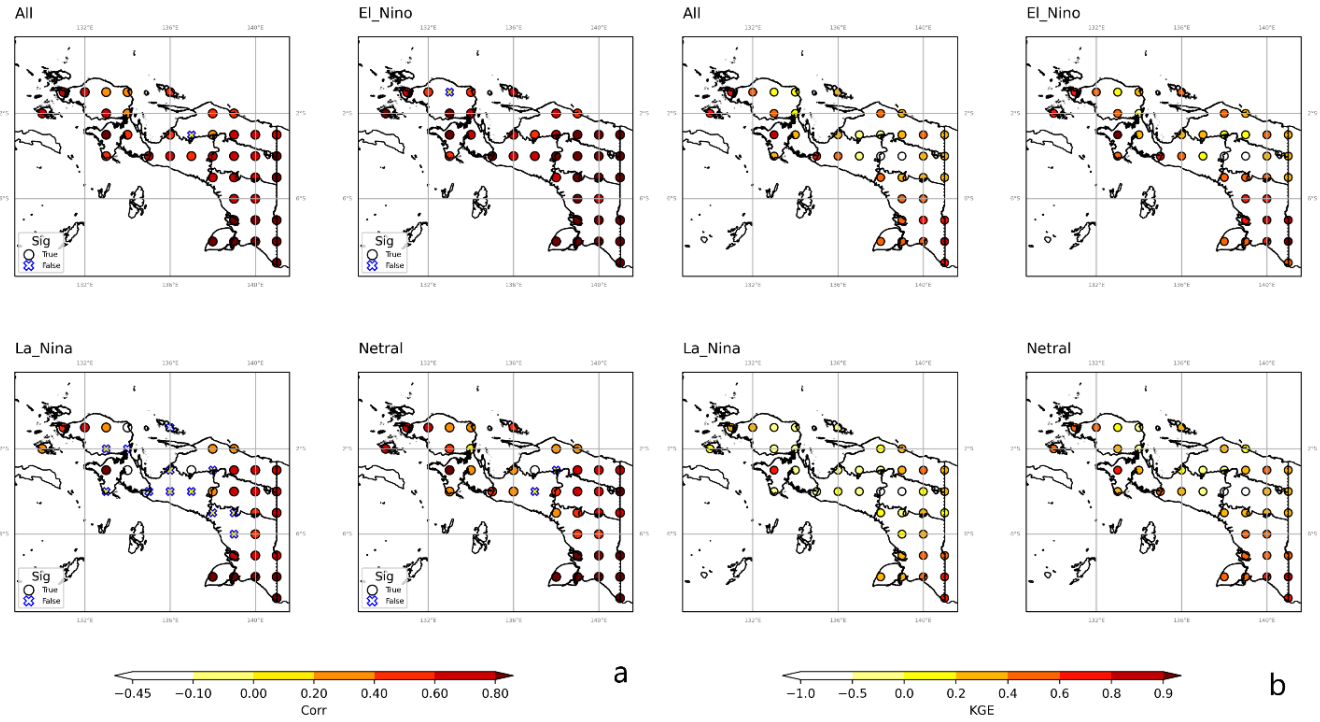

Figure 3 Seasonal performance of 3-month moving average of SEAS5 and CHIRP+Pos for each ENSO phases (a) Correlation; (b) Kling-Gupta Error (KGE). Shade showed metrics value with 'o' denotated significant value and 'x' is non-significant value for correlation.

average values >0.60 and >0.4, respectively. These patterns align with prior studies reporting strong ENSO influences in the Maritime Continent (Kurniadi et al., 2021; Hidayat et al., 2025) yielding dry and wet anomalies particularly in Papua (Supari et al., 2018). This pattern is consistent with seasonal assessments, reflecting SEAS5's forecast skill underperformed during wet condition with wet biases more pronounced (Ehsan et al., 2021). Regions with strong relationship with ENSO exhibited higher performance for SEAS5's precipitation model (Gubler et al., 2020).

In addition, the SEAS5's forecast skill showed good performances in lowland areas during El-Niño compared to La Niña and Neutral conditions. The correlation peaked at 0.97 in lowland with only one non-significant grid during El Niño. In contrast, La Niña phases show numerous non-significant (30%) grids predominantly in mountainous regions and the west coast of Papua. Despite strong correlation in some high-elevation grids, low KGE (e.g., < -0.41, marked by white 'o' in Figure 3b) and high RMSE indicate large errors and bias, rendering SEAS5 less skillful than the climatological mean in these regions.

SEAS5's performance across El Niño, La Niña, and Neutral phases at lead times 1, 2, and 3 months also observed by boxplots (Figure 7), highlighting variability in Corr, KGE, and RMSE. La Niña consistently shows wider interquartile ranges (IQR) for Corr and KGE compared to El Niño and Neutral phases, with this instability become more pronounced at longer lead times as the metric distributions broaden. This suggests greater variability in predictive skill during La Niña, potentially linked to challenges in modeling certain conditions, as evidenced by outliers where KGE drops below -0.41 (Figure 3b). In contrast, El Niño displays narrower IQRs, reflecting more stable performance, particularly at lead time 1, with Corr reaching up to 0.973. The increasing variability at extended lead times, especially for La Niña, may point to limitations in capturing regional dynamics, a pattern consistent with the model's struggles in high-elevation areas as noted in Figure 3, a limitation that will be discussed later. Compared to the climatology, SEAS5 performs better during El Niño (based on KGE score), aligning with findings of enhanced predictability in dry conditions (Palmer et al., 2004; Zhang et al., 2016; Abid et al., 2018; Ferreira et al., 2022). These insights underscore the need for refined parameterization to address lead-time and phase-specific challenges across Papua.

To illustrate SEAS5's performance across ENSO phases, we analyzed time series of SEAS5 prediction along with CHIRP+Pos observation during strong El Niño (1982, 1997, 2015), La Niña (1988, 1998, 2010), and Neutral condition (1989, 1993, 2001) following classification of (Supari et al., 2018). We selected 3 grids with contradictory metrics, strong Corr but low KGE and high RMSE mentioned above, located in highlands depicted inside red boxes in Figure 3 (com-

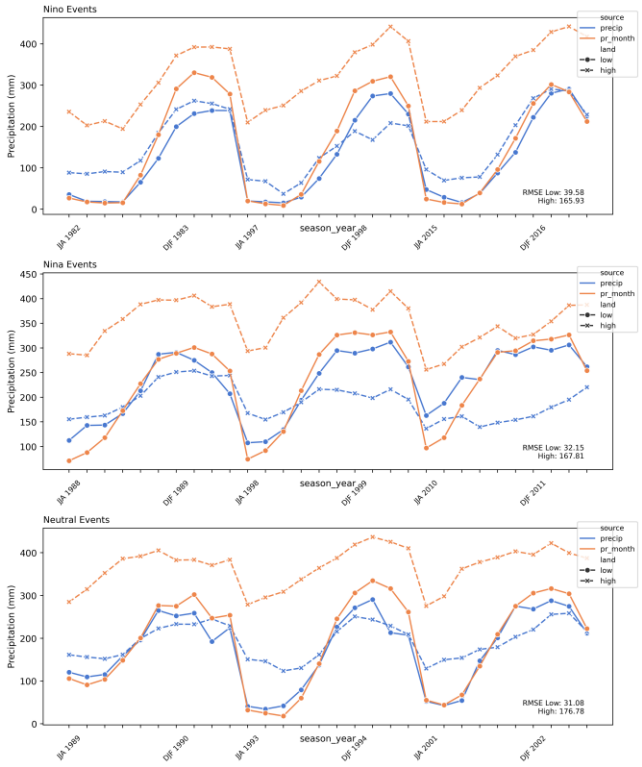

Figure 4 Time series of SEAS5 prediction (orange line) with CHIRP+Pos (blue) on El-Niño (top), La-Niña (middle), Neutral (bottom) event. Dotted solid line represents rainfall in lowlands, while dashed-line with 'x' represents rainfall in highlands

pared it with Figure 1 for elevation context), and compared them to 3 grids with consistent good metrics in lowland areas in southern Papua (blue boxes in Figure 3). These grids were respectively averaged to produce time series shown in Figure 4.

The results show that SEAS5 consistently follows the pattern of rainfall in lowlands on all ENSO phases, closer alignment during El Niño compared to La Niña and Neutral condition. SEAS5 rainfall in lowland areas showed a slight overestimation, whereas in highland areas the average rainfall was nearly two times greater than that of CHIRP+Pos. The rainfall SEAS5 on highlands resembles the pattern of rainfall but with much larger RMSE compared to lowlands, roughly 4 times larger compared to RMSE in lowlands (RMSE of 165.9 mm in highlands, 39.6 mm in lowlands). The elevated errors contribute to low KGE scores and outliers observed in boxplots from Figure 6 and Figure 7. This case study further highlights SEAS5's stronger performance in producing more accurate rainfall prediction in lowlands while underscoring SEAS5's challenge in highlands.

3.3 Performance Over Lead Time

The SEAS5's performance was evaluated by correlations, KGE, and RMSE with three different lead times (1, 2, and 3 months) for each ENSO phase as shown in Figure 8. All metrics consistently showed better performance of SEAS5 in all, El-Niño, and neutral conditions compared to La-Niña, which has the highest rainfall variability (Supari et al., 2018). Correlation values were high in all, El-Niño and neutral condition with more than 0.5, while in La-Niña showed the lowest with mean value < 0.5 and longer Inter-Quantile Range (IQR). The same pattern was found in KGE results, La-Niña has the lowest mean value < 0.25, compared to other conditions which ranges from 0.25-0.50. The wider IQR indicating greater instability, especially during La Niña (Kowal et al., 2022). In RMSE, all conditions established low value, including La-Niña which ranges from 50-125, very similar for each lead time. This suggests challenges in predicting wet anomalies, with potential outliers reflecting the model's limitations in high-terrain areas (compared to Figure 3).

Generally, the results showed, performance declined as lead times increased, align with previous study (Chevuturi et al., 2021). Correlation and KGE are consistent showing 1 month lead time has the highest mean value while 3-month lead time showed the lowest. Unique pattern was found in RMSE, all lead times showed similar mean value and IQR, indicates there is no significant difference. These reflecting redu-ced predictive skill as lead times increased (Kowal et al., 2022), even when post-process-ing technique were applied (Yang et al., 2017; Ratri et al., 2023). These findings underscore SEAS5's suitability for short-term forecasts in lowland Papua, highlighting the need for improved parameterization to address lead-time and topographic challenges across the region.

3.4 Relationship of Topography and SEAS5 Performance

The relationship of topography and SEAS5 performance was observed by statistical metrics from linear regression between calculated RMSE (y) and elevation data (x) as shown in Table 2. The result showed that elevation statistically affect RMSE in Papua with p-value lower than 0.001% for all lead times. Slope showed that with 100 m increases of elevation, RMSE grows 3.99 to 3.53 mm/month. The result showed that elevation explain up to 48% variance of the regression model, de-

Table 2 Regression results between RMSE (y) and elevation (x) for each lead time

Slope	R^2	Lead time	Significance P
0.039	0.482	1	< 0.001
0.036	0.450	2	< 0.001
0.035	0.452	3	< 0.001

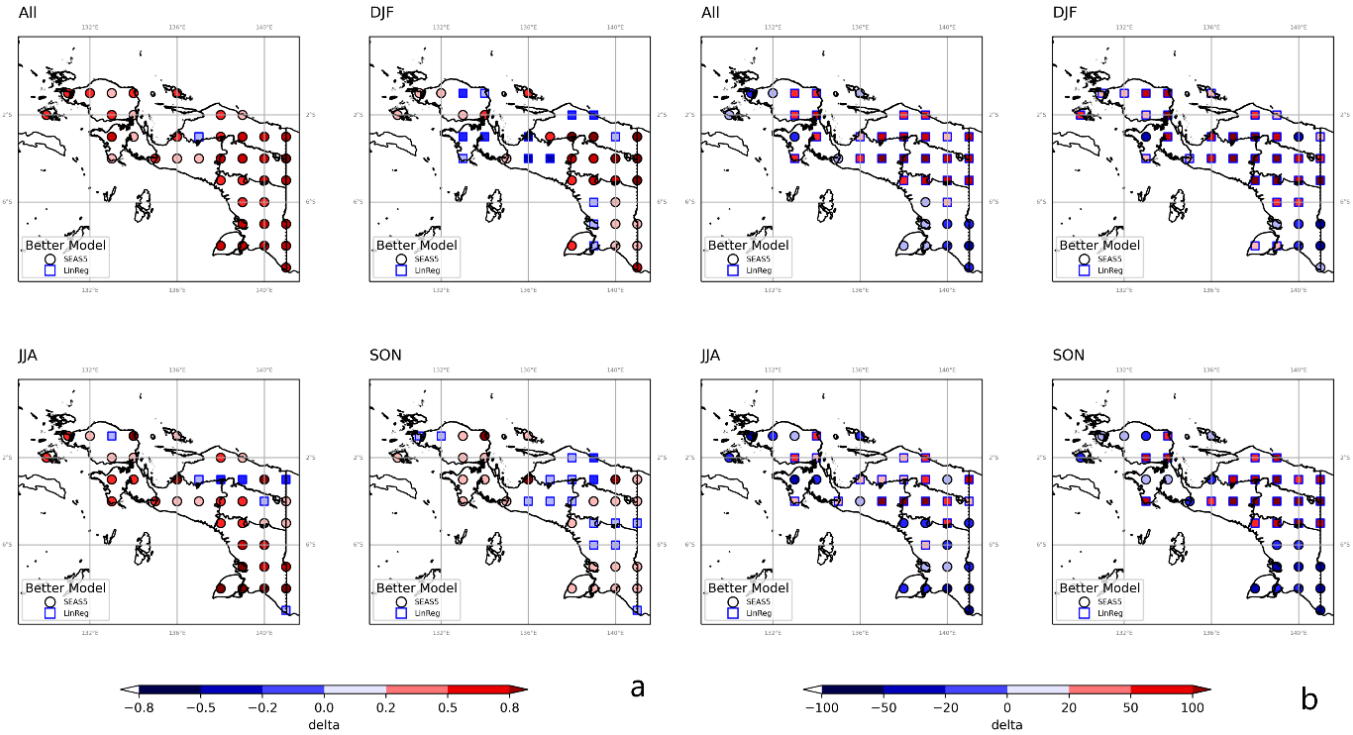

Figure 5 Comparison of SEAS5 and linear regression as baseline model in Papua calculated by difference value of SEAS5 and baseline in (a) Correlation (Corr) and (b) Root Mean Squared Error (RMSE)

creasing with longer lead time. This relationship also confirmed by previous study where rainfall likely to have largest errors on mountainous area (Hidayat and Taufik, 2025) and study in Central America, elevation in Papua affects prediction skill more (Kowal et al., 2022).

3.5 Comparison between SEAS5 and Baseline Model

The SEAS5 performance also assessed by comparing the predictive model baseline model constructed using simple linear regression to assess its predictive skill using 3-month lagged ONI index (Figure 5). The comparison was based on correlation and RMSE. Differences were calculated by subtracting SEAS5's metric with baseline. The positive differences in correlation indicate that SEAS5 is better at capturing rainfall pattern, while negative differences in RMSE reflect SEAS5's prediction error relative to the baseline. This benchmarking provides a reference to assess SEAS5 performance against a simple real-life method of rainfall prediction in Papua.

The seasonal benchmarking analysis reveals that SEAS5 predictions align with observed rainfall patterns in 76.2% of grids across Papua, outperforming the baseline model, as indicated by positive difference of Corr (Figure 5a), where 'o' markers denote grids where SEAS5 excels. Seasonal variations of performance are notable: SEAS5 achieved the highest proportion of grids with stronger Corr during JJA (82.5%), reflecting a robust ENSO-rainfall teleconnection. A similar result was reported in Central America, where SEAS5 performed best on July-October (Kowal et al., 2022). In contrast, SEAS5 outperformed the baseline in only 60% of grids during SON, the lowest among all periods, suggesting that its skill is not solely driven by ENSO-related variability, aligning with (Gubler et al., 2020). SEAS5 consistently give better Corr relative to the baseline particularly in lowland areas in western and southern Papua.

Despite SEAS5's strong performance in capturing rainfall patterns, SEAS5's limitations are evident in the RMSE metric benchmarking (Figure 5b), where the baseline model yielded lower RMSE in 60.6% of grids, marked by squares indicating baseline superiority. During the DJF season, only 20% of grids exhibited lower RMSE for SEAS5. SEAS5 consistently yields lower RMSE values compared to the baseline in southern lowland areas. These results underscore the importance of using multiple metrics for model evaluation, as SEAS5 excels in capturing rainfall patterns (Corr) but struggles with prediction errors (RMSE). Consequently, in areas where minimizing errors is prioritized over capturing patterns, the baseline model is often preferable across Papua.

These findings confirm SEAS5's ability to capture large-scale rainfall patterns in Papua, consistent with the time series analysis in previous section (Figure 4). However, significant errors, particularly in high-elevation areas, allow a simpler baseline model to achieve lower RMSE, supporting prior evidence that

statistical models can outperform dynamical forecasts in certain contexts (Rodrigues et al., 2014).

4. CONCLUSION

This study assessed ECMWF SEAS5 rainfall predictions in Papua across seasons and ENSO phases, revealing better predictive skill on JAS - SON compared to skill in DJF - JFM, showing challenges in predicting boreal winter rainfall. The model exhibited superior performance during El Niño phase, particularly in lowlands, but showed greater variability and lower skill during La Niña and Neutral phases, as evidenced by wider IQR for Corr and KGE. SEAS5's limitations were evident in high-elevation areas, indicated by much larger RMSE on highlands as illustrated by time series analysis and KGE score below -0.41, indicating performance inferior to climatological mean. Increase in elevation statistically increased model's error.

Despite these limitations, SEAS5's ability to capture rainfall patterns in lowland regions supports its utility for climate risk management, particularly for drought preparedness in areas like Merauke, where El Niño-induced droughts correlate with burned area. The inherent uncertainty in seasonal forecasts, evidenced by wider IQR of metrics during La Niña and DJF underscores the need for cautious interpretation when applying SEAS5 outputs for agricultural planning or flood mitigation. Future study should focus on applying various statistical post-processing techniques demonstrated to enhance GCM's predictive skill.

ACKNOWLEDGEMENT

This study was supported and funded by Indonesia Endowment Fund for Education Agency (LPDP) - The Ministry of Finance Republic Indonesia. The authors thank Indonesia Agency for Meteorology Climatology and Geophysics (BMKG), and Mr. Robi Muharsyah in particular, for providing the CHIRP+Pos dataset used in this study.

REFERENCES

Abid, M.A., Almazroui, M., Kucharski, F., O'Brien, E., Yousef, A.E., 2018. ENSO relationship to summer rainfall variability and its potential predictability over Arabian Peninsula region. npj Clim Atmos Sci 1, 1–7. https://doi.org/10.1038/s41612-017-0003-7

Aldrian, E., Dümenil Gates, L., Widodo, F.H., 2007. Seasonal variability of Indonesian rainfall in ECHAM4 simulations and in the reanalyses: The role of ENSO. Theor. Appl. Climatol. 87, 41–59. https://doi.org/10.1007/s00704-006-0218-8

Aldrian, E., Dwi Susanto, R., 2003. Identification of three dominant rainfall regions within Indonesia and their relationship to sea surface temperature. International Journal of Climatology 23, 1435–1452. https://doi.org/10.1002/joc.950

Ariyani, D., Perdinan, Purwanto, M.Y.J., Sunarti, E., Juniati, A.T., Ibrahim, M., 2023. Contributed Indicators to Fluvial Flood Along River Basin in Urban Area of Indonesia. Geography, Environment, Sustainability 15, 102–114. https://doi.org/10.24057/2071-9388-2022-084

As-syakur, Abd.R., Adnyana, I.W.S., Mahendra, M.S., Arthana, I.W., Merit, I.N., Kasa, I.W., Ekayanti, N.W., Nuarsa, I.W., Sunarta, I.N., 2014. Observation of spatial patterns on the rainfall response to ENSO and IOD over Indonesia using TRMM Multisatellite Precipitation Analysis (TMPA). International Journal of Climatology 34, 3825–3839. https://doi.org/10.1002/joc.3939

Buontempo, C., Burgess, S.N., Dee, D., Pinty, B., Thépaut, J.-N., Rixen, M., Almond, S., Armstrong, D., Brookshaw, A., Alos, A.L., Bell, B., Bergeron, C., Cagnazzo, C., Comyn-Platt, E., Damasio-Da-Costa, E., Guillory, A., Hersbach, H., Horányi, A., Nicolas, J., Obregon, A., Ramos, E.P., Raoult, B., Muñoz-Sabater, J., Simmons, A., Soci, C., Suttie, M., Vamborg, F., Varndell, J., Vermoote, S., Yang, X., Garcés De Marcilla, J., 2022. The Copernicus Climate Change Service: Climate Science in Action. Bulletin of the American Meteorological Society 103, E2669–E2687. https://doi.org/10.1175/BAMS-D-21-0315.1

Chai, T., Draxler, R.R., 2014. Root mean square error (RMSE) or mean absolute error (MAE)? – Arguments against avoiding RMSE in the literature. Geosci. Model Dev. 7, 1247–1250. https://doi.org/10.5194/gmd-7-1247-2014

Chevuturi, A., Turner, A.G., Johnson, S., Weisheimer, A., Shonk, J.K.P., Stockdale, T.N., Senan, R., 2021. Forecast skill of the Indian monsoon and its onset in the ECMWF seasonal forecasting system 5 (SEAS5). Clim Dyn 56, 2941–2957. https://doi.org/10.1007/s00382-020-05624-5

Daymond, A.J., Prawoto, A., Abdoellah, S., Susilo, A.W., Cryer, N.C., Lahive, F., Hadley, P., 2020. Variation in Indonesian cocoa farm productivity in relation to management, environmental and edaphic factors. Experimental Agriculture 56, 738–751. https://doi.org/10.1017/S0014479720000289

Ehsan, M.A., Tippett, M.K., Robertson, A.W., Almazroui, M., Ismail, M., Dinku, T., Acharya, N., Siebert, A., Ahmed, J.S., Teshome, A., 2021. Seasonal predictability of Ethiopian Kiremt rainfall and forecast skill of ECMWF's SEAS5 model. Clim

Dyn 57, 3075–3091. https://doi.org/10.1007/s00382-021-05855-0

Ferreira, G.W.S., Reboita, M.S., Drumond, A., 2022. Evaluation of ECMWF-SEAS5 Seasonal Temperature and Precipitation Predictions over South America. Climate 10, 128. https://doi.org/10.3390/cli10090128

Firmansyah, A.J., Nurjani, E., Sekaranom, A.B., 2022. Effects of the El Niño-Southern Oscillation (ENSO) on rainfall anomalies in Central Java, Indonesia. Arab J Geosci 15, 1746. https://doi.org/10.1007/s12517-022-11016-2

Funk, C., Peterson, P., Landsfeld, M., Pedreros, D., Verdin, J., Shukla, S., Husak, G., Rowland, J., Harrison, L., Hoell, A., Michaelsen, J., 2015. The climate hazards infrared precipitation with stations—a new environmental record for monitoring extremes. Sci Data 2, 150066. https://doi.org/10.1038/sdata.2015.66

Gubler, S., Sedlmeier, K., Bhend, J., Avalos, G., Coelho, C. a. S., Escajadillo, Y., Jacques-Coper, M., Martinez, R., Schwierz, C., Skansi, M. de, Spirig, C., 2020. Assessment of ECMWF SEAS5 Seasonal Forecast Performance over South America. Weather and Forecasting 35, 561–584. https://doi.org/10.1175/WAF-D-19-0106.1

Gupta, H.V., Kling, H., Yilmaz, K.K., Martinez, G.F., 2009. Decomposition of the mean squared error and NSE performance criteria: Implications for improving hydrological modelling. Journal of Hydrology 377, 80–91. https://doi.org/10.1016/j.jhydrol.2009.08.003

Harris, C.R., Millman, K.J., van der Walt, S.J., Gommers, R., Virtanen, P., Cournapeau, D., Wieser, E., Taylor, J., Berg, S., Smith, N.J., Kern, R., Picus, M., Hoyer, S., van Kerkwijk, M.H., Brett, M., Haldane, A., del Río, J.F., Wiebe, M., Peterson, P., Gérard-Marchant, P., Sheppard, K., Reddy, T., Weckesser, W., Abbasi, H., Gohlke, C., Oliphant, T.E., 2020. Array programming with NumPy. Nature 585, 357–362. https://doi.org/10.1038/s41586-020-2649-2

Hidayat, R., Apip, Dasril, A.P., Taufik, M., 2025. Climate teleconnection triggers prolonged dry season in tropical maritime continent. Theoretical and Applied Climatology 156, 626. https://doi.org/10.1007/s00704-025-05852-x

Hidayat, R., Taufik, M., 2025. Bias Correction of CMIP6 Models for Assessment of Wet and Dry Conditions Over Sumatra. Agromet 39, 33–39. https://doi.org/10.29244/j.agromet.39.1.33-39

Hoyer, S., Hamman, J., 2017. xarray: N-D labeled Arrays and Datasets in Python. Journal of Open Research Software 5. https://doi.org/10.5334/jors.148

Huang, B., Thorne, P.W., Banzon, V.F., Boyer, T., Chepurin, G., Lawrimore, J.H., Menne, M.J., Smith, T.M., Vose, R.S., Zhang, H.-M., 2017. Extended Reconstructed Sea Surface Temperature, Version 5 (ERSSTv5): Upgrades, Validations, and Intercomparisons. Journal of Climate 30, 8179–8205. https://doi.org/10.1175/JCLI-D-16-0836.1

Irawan, A.N.R., Komori, D., Hendrawan, V.S.A., 2023. Correlation analysis of agricultural drought risk on wet farming crop and meteorological drought index in the tropical-humid region. Theor Appl Climatol 153, 227–240. https://doi.org/10.1007/s00704-023-04461-w

Johnson, S.J., Stockdale, T.N., Ferranti, L., Balmaseda, M.A., Molteni, F., Magnusson, L., Tietsche, S., Decremer, D., Weisheimer, A., Balsamo, G., Keeley, S.P.E., Mogensen, K., Zuo, H., Monge-Sanz, B.M., 2019a. SEAS5: the new ECMWF seasonal forecast system. Geoscientific Model Development 12, 1087–1117. https://doi.org/10.5194/gmd-12-1087-2019

Johnson, S.J., Stockdale, T.N., Ferranti, L., Balmaseda, M.A., Molteni, F., Magnusson, L., Tietsche, S., Decremer, D., Weisheimer, A., Balsamo, G., Keeley, S.P.E., Mogensen, K., Zuo, H., Monge-Sanz, B.M., 2019b. SEAS5: the new ECMWF seasonal forecast system. Geosci. Model Dev. 12, 1087–1117. https://doi.org/10.5194/gmd-12-1087-2019

Knoben, W.J.M., Freer, J.E., Woods, R.A., 2019. Technical note: Inherent benchmark or not? Comparing Nash–Sutcliffe and Kling–Gupta efficiency scores. Hydrology and Earth System Sciences 23, 4323–4331. https://doi.org/10.5194/hess-23-4323-2019

Kowal, K.M., Slater, L.J., Van Loon, A.F., Birkel, C., 2022. SEAS5 skilfully predicts late wet-season precipitation in Central American Dry Corridor excelling in Costa Rica and Nicaragua. International Journal of Climatology 42, 4953–4971. https://doi.org/10.1002/joc.7514

Kurniadi, A., Weller, E., Min, S.-K., Seong, M.-G., 2021. Independent ENSO and IOD impacts on rainfall extremes over Indonesia. International Journal of Climatology 41, 3640–3656. https://doi.org/10.1002/joc.7040

Muharsyah, R., 2020. Perbandingan Model Kopel ECMWF System 4 Dan CFSV2 Untuk Prediksi Musim Di Indonesia. Buletin Meteorologi, Klimatologi, Geofisika, dan Kualitas Udara 11,

1–11. https://doi.org/10.46824/megasains.v11i01.3

Mulsandi, A., Koesmaryono, Y., Hidayat, R., Faqih, A., Sopaheluwakan, A., 2024. Detecting Indonesian Monsoon Signals and Related Features Using Space–Time Singular Value Decomposition (SVD). Atmosphere 15, 187. https://doi.org/10.3390/atmos15020187

Muntohar, A.S., Ikhsan, J., Liao, H.-J., Jotisankasa, A., Jetten, V.G., 2022. Rainfall Infiltration-induced Slope Instability of the Unsaturated Volcanic Residual Soils During Wet Seasons in Indonesia. Indonesian Journal on Geoscience 9, 71–85. https://doi.org/10.17014/ijog.9.1.71-85

Nurdiati, S., Bukhari, F., Sopaheluwakan, A., Septiawan, P., Hutapea, V., 2023. ENSO and IOD Impact Analysis of Extreme Climate Condition in Papua, Indonesia. GT 19, 1–18. https://doi.org/10.21163/GT_2024.191.01

Palmer, T.N., Alessandri, A., Andersen, U., Cantelaube, P., Davey, M., Délécluse, P., Déqué, M., Díez, E., Doblas-Reyes, F.J., Feddersen, H., Graham, R., Gualdi, S., Guérémy, J.-F., Hagedorn, R., Hoshen, M., Keenlyside, N., Latif, M., Lazar, A., Maisonnave, E., Marletto, V., Morse, A.P., Orfila, B., Rogel, P., Terres, J.-M., Thomson, M.C., 2004. Development of A European Multimodel Ensemble System for Seasonal-to-Interannual Prediction (Demeter). Bulletin of the American Meteorological Society 85, 853–872. https://doi.org/10.1175/BAMS-85-6-853

Pangau-Adam, M.Z., Brodie, J.F., 2019. Threats to the populations of two endemic brushturkey species in Indonesian New Guinea. Journal of Asia-Pacific Biodiversity 12, 488–492. https://doi.org/10.1016/j.japb.2019.07.005

Permana, D.S., Thompson, L.G., Setyadi, G., 2016. Tropical West Pacific moisture dynamics and climate controls on rainfall isotopic ratios in southern Papua, Indonesia. Journal of Geophysical Research: Atmospheres 121, 2222–2245. https://doi.org/10.1002/2015JD023893

Prentice, M., Hope, G., 2007. Climate of Papua, in: The Ecology of Papua: Part One. Periplus Editions, Singapore, pp. 177–195.

Rahayu, R., Mathias, S.A., Reaney, S., Vesuviano, G., Suwarman, R., Ramdhan, A.M., 2023. Impact of land cover, rainfall and topography on flood risk in West Java. Nat Hazards 116, 1735–1758. https://doi.org/10.1007/s11069-022-05737-6

Ratri, D.N., Weerts, A., Muharsyah, R., Whan, K., Tank, A.K., Aldrian, E., Hariadi, M.H., 2023. Calibration of ECMWF SEAS5 based streamflow forecast in Seasonal hydrological forecasting for Citarum river basin, West Java, Indonesia. Journal of Hydrology: Regional Studies 45, 101305. https://doi.org/10.1016/j.ejrh.2022.101305

Robertson, A.W., Moron, V., Qian, J.-H., Chang, C.-P., Tangang, F., Aldrian, E., Koh, T.Y., Liew, J., 2011. The maritime continent monsoon, in: The Global Monsoon System, World Scientific Series on Asia-Pacific Weather and Climate. WORLD SCIENTIFIC, pp. 85–98. https://doi.org/10.1142/9789814343411_0006

Rodrigues, L.R.L., García-Serrano, J., Doblas-Reyes, F., 2014. Seasonal forecast quality of the West African monsoon rainfall regimes by multiple forecast systems. Journal of Geophysical Research: Atmospheres 119, 7908–7930. https://doi.org/10.1002/2013JD021316

Sugianti, K., Yunarto, Y., Sadisun, I., Kartiko, R., 2022. Analysis of Maximum-Rainfall-Infiltration-Induced Slope Stability Using the Transient Rainfall Infiltration and Grid-based Regional Slope-stability Model in Cililin, West Java, Indonesia. Indonesian Journal on Geoscience 9, 263–278. https://doi.org/10.17014/ijog.9.2.263-278

Supari, Tangang, F., Salimun, E., Aldrian, E., Sopaheluwakan, A., Juneng, L., 2018. ENSO modulation of seasonal rainfall and extremes in Indonesia. Clim Dyn 51, 2559–2580. https://doi.org/10.1007/s00382-017-4028-8

Viandari, N.A., Wihardjaka, A., Pulunggono, H.B., Suwardi, S., 2022. Sustainable Development Strategies of Rainfed Paddy Fields in Central Java, Indonesia: A Review. Caraka Tani: Journal of Sustainable Agriculture 37, 275–288. https://doi.org/10.20961/carakatani.v37i2.58242

Villafuerte, M.Q., Matsumoto, J., 2015. Significant Influences of Global Mean Temperature and ENSO on Extreme Rainfall in Southeast Asia. Journal of Climate 28, 1905–1919. https://doi.org/10.1175/JCLI-D-14-00531.1

Wang, Y., Gueye, M., Greybush, S.J., Greatrex, H., Whalen, A.J., Ssentongo, P., Zhang, F., Jenkins, G.S., Schiff, S.J., 2023. Verification of operational numerical weather prediction model forecasts of precipitation using satellite rainfall estimates over Africa. Meteorological Applications 30, e2112. https://doi.org/10.1002/met.2112

Wu, P., Arbain, A.A., Mori, S., Hamada, J., Hattori, M., Syamsudin, F., Yamanaka, M.D., 2013. The Effects of an Active Phase of the Madden-Julian Oscillation on the Extreme Precipitation Event over Western Java Island in January 2013. Sola.

9, 79–83. https://doi.org/10.2151/sola.2013-018

Yang, X., Sharma, S., Siddique, R., Greybush, S.J., Mejia, A., 2017. Postprocessing of GEFS Precipitation Ensemble Reforecasts over the U.S. Mid-Atlantic Region. Monthly Weather Review 145, 1641–1658. https://doi.org/10.1175/MWR-D-16-0251.1

Zhang, T., Yang, S., Jiang, X., Zhao, P., 2016. Seasonal–Interannual Variation and Prediction of Wet and Dry Season Rainfall over the Maritime Continent: Roles of ENSO and Monsoon Circulation. Journal of Climate 29, 3675–3695. https://doi.org/10.1175/JCLI-D-15-0222.1

ANNEX

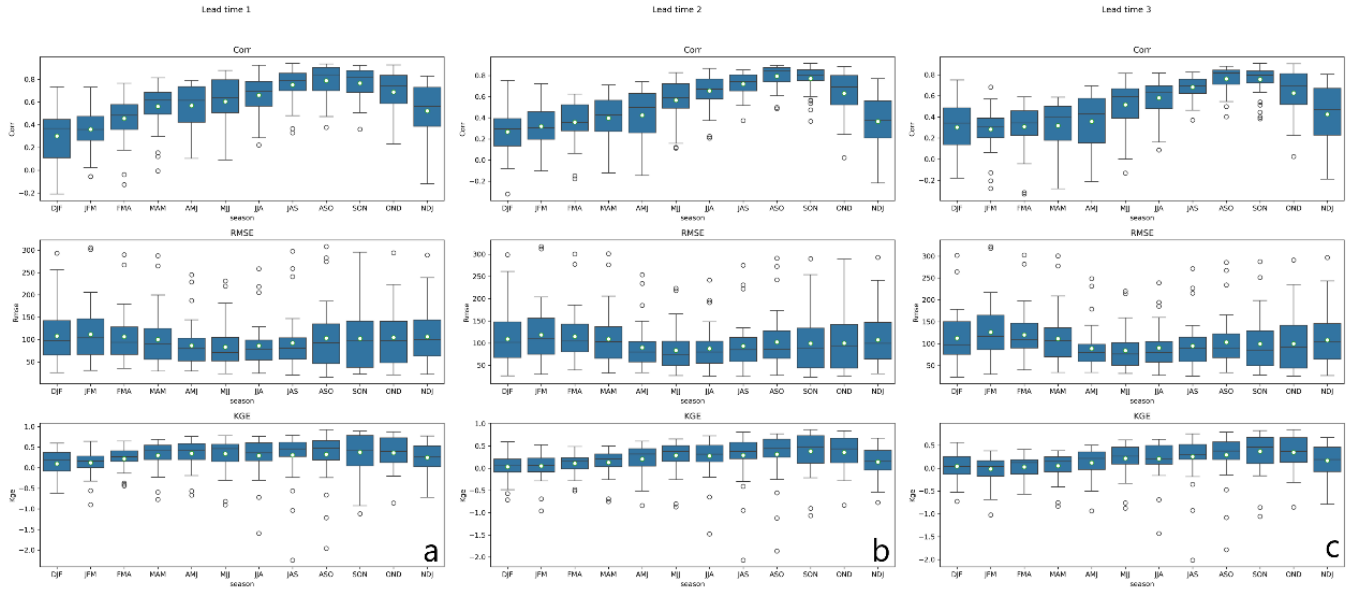

Figure 6 Seasonal performance of correlation (top row), Root Mean Squared Error (middle row), and Kling-Gupta Error (bottom row) for (a) 1-month; (b) 2-months; and (c) 3-months lead time

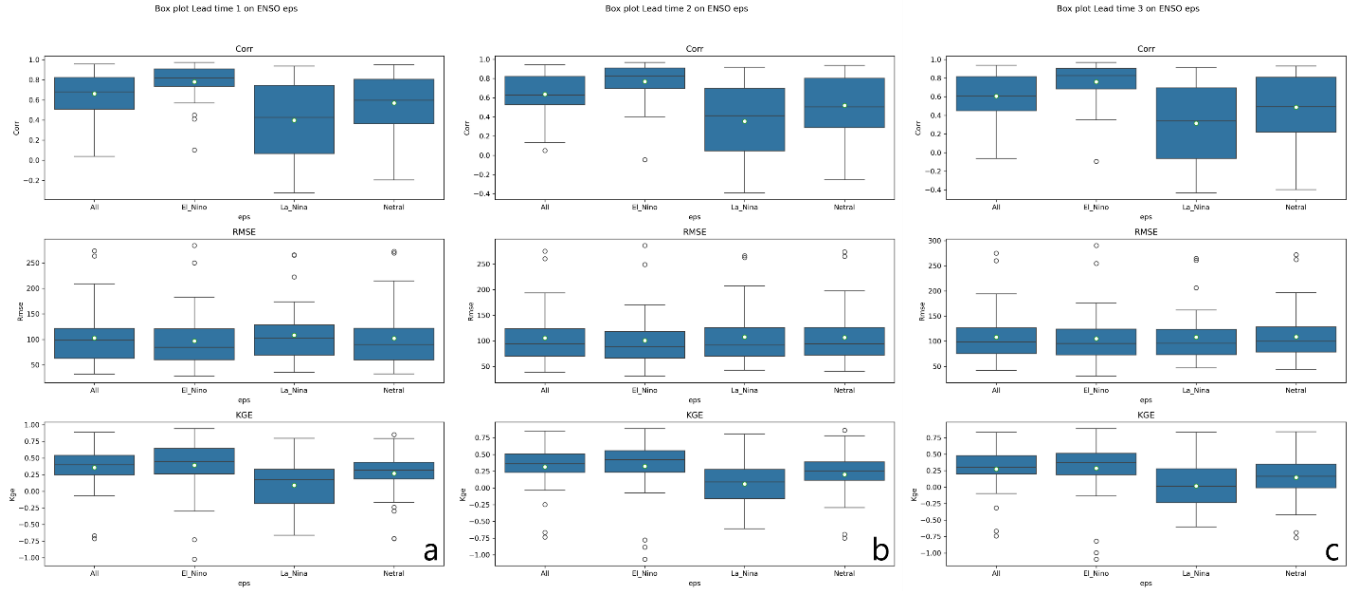

Figure 7 ENSO-phase performances of correlation (top row), Root Mean Squared Error (middle row), and Kling-Gupta Error (bottom row) for (a) 1-month; (b) 2-months; and (c) 3-months lead time

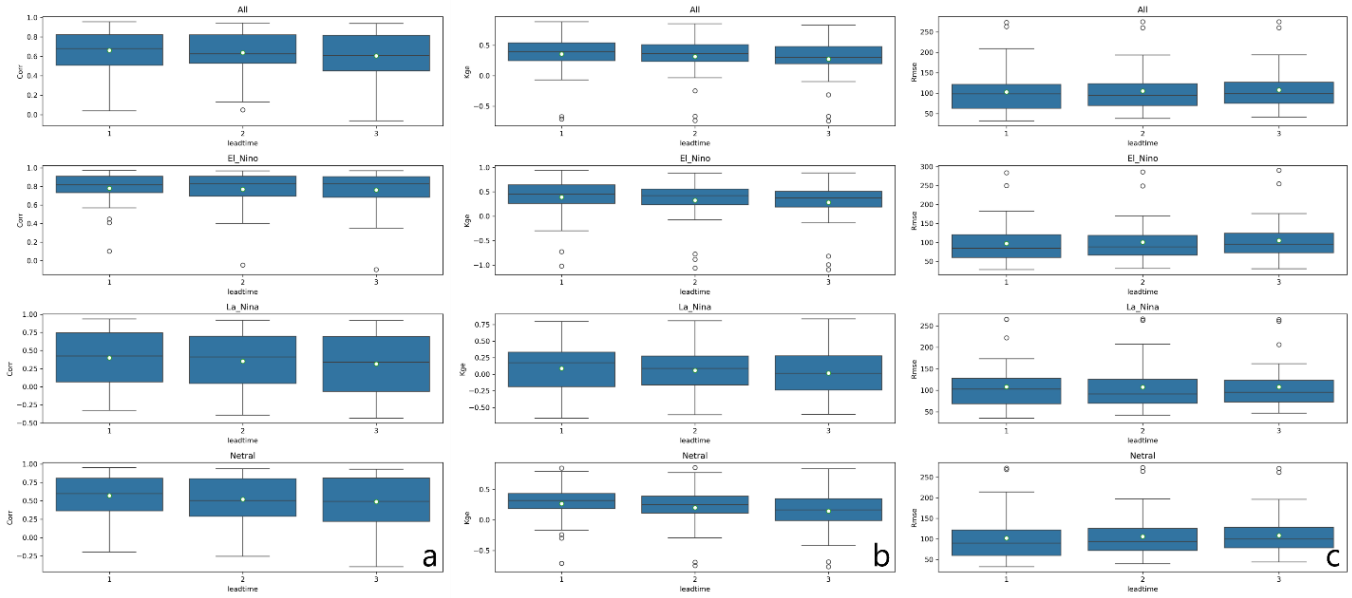

Figure 8 SEAS5's performances of correlation (top row), Root Mean Squared Error (middle row), and Kling-Gupta Error (bottom row) for (a) 1-month; (b) 2-months; and (c) 3-months lead time